

About the TATB hypothesis: solvation of the $\text{As}\phi_4^+$ and $\text{B}\phi_4^-$ ions and their tetrahedral and spherical analogues in aqueous/nonaqueous solvents and at a water–chloroform interface†

Rachel Schurhammer and Georges Wipff*

Laboratoire de Modelisation et Simulations Moléculaire (CNRS UMR 7551), Université Louis Pasteur, Institut de Chimie, 4 rue B. Pascal, 67 000 Strasbourg, France.

E-mail: wipff@chimie.u-strasbg.fr

Received (in Montpellier, France) 15th January 1999, Accepted 11th February 1999

Based on molecular dynamics (MD) and free energy (FEP) simulations, we investigate the effect of $+/-$ charge on the solvation properties of large “symmetrical” ions in water, acetonitrile and chloroform solutions. The nearly isostructural $\text{As}\phi_4^+$ and $\text{B}\phi_4^-$ tetrahedral ions, which have been assumed to display identical energies of transfer from water to any solvent (“TATB hypothesis”), are found to display marked differences in solution. The anion interacts more than the cation with water, chloroform and acetonitrile, due to short-range electrostatic interactions, in relation to the solvent granularity and shape of the ion. The importance of charge distribution is demonstrated by the simulations on four different models of $\text{As}\phi_4^+$ and $\text{B}\phi_4^-$, on fictitious $\text{B}\phi_4^+$ and $\text{As}\phi_4^-$ ions, and on neutral $\text{B}\phi_4^0$ and $\text{As}\phi_4^0$ analogues. The role of ion shape is demonstrated by MD and FEP simulations on isovolumic spherical S^+ and S^- ions, which also display marked differences in solvation properties, but opposite to those of $\text{As}\phi_4^+$ and $\text{B}\phi_4^-$. In water, S^+ is much better hydrated than S^- , due to clathrate-type hydration around S^+ , while in acetonitrile, S^+ and S^- display similar solvation energies. The question of ion pairing is also examined in the three solvents. At a liquid–liquid water–chloroform interface represented explicitly, the $\text{B}\phi_4^-$ anion is found to be more surface active than $\text{As}\phi_4^+$. A number of methodological issues are addressed in the paper. These results are important in the context of the TATB hypothesis and for our understanding of solvation of large hydrophobic ions in pure liquids or in heterogeneous environments like aqueous interfaces.

The precise determination of solvation properties of electrolytes represents a problem of utmost importance in physical chemistry. An inherent difficulty in this problem is our inability to measure *individual* solvation energies of ions,¹ corresponding to their transfer from a fixed point in the gas phase to a fixed point in solution.² Experiments provide thermodynamic solvation functions of salts, which are generally assumed to be the *sum* of the cation and anion contributions, but assignment of individual ion contributions rests on “extrathermodynamic assumptions”, pioneered by Bjerrum and Larsson in 1927.³ As reviewed by Kim⁴ and Marcus,^{5,6} the most widely practiced method is “based on the assumption that the medium effect for a large reference cation can be equated to that of a reference anion of molecular similarity”. After the introduction of $\text{P}\phi_4^+\text{B}\phi_4^-$ as a reference electrolyte by Grunwald *et al.*,⁷ other pairs of reference ions were suggested, involving the TAB^+ quaternary ammonium (TAB^+ = triisomyl-*n*-butylammonium⁸) or TA^+ (TA = tetraphenylarsonium $\text{As}\phi_4^+$ ⁹) cations and the $\text{B}\phi_4^-$ anion. It is indeed generally assumed that bulk cations and anions of the same charge display similar solvation properties in pure aqueous or in mixed water–liquid solvents.⁷ According to the TATB (TATB = TetraphenylArsonium TetraphenylBorate) hypothesis^{5,10} $\text{As}\phi_4^+$ and the $\text{B}\phi_4^-$ anion have the same free energy of transfer from water to *any solvent* s :

$$\Delta G_{\text{wat} \rightarrow s}(\text{As}\phi_4^+) = \Delta G_{\text{wat} \rightarrow s}(\text{B}\phi_4^-) = 1/2 \Delta G_{\text{wat} \rightarrow s}(\text{As}\phi_4\text{B}\phi_4) \quad (1)$$

Based on this hypothesis, the free energies of transfer of single anions and single cations from water to all kinds of solvents (polar/apolar, protic/aprotic, *etc.* ...) have been put on the same scale.⁵ According to Marcus, this reference electrolyte concept “depends on the expectations that the interactions of its cation and its anion with their solvent environments should be *equal* and *independent of the sign of the charge*, provided that these ions meet certain criteria. These are that the ions should (i) have unit charge, (ii) be similar in most respects, (iii) have the same size, (iv) be very large, (v) be as nearly spherical as possible and (vi) have an inert periphery”.¹⁰ Free energies of solvation involve solute–solvent and solvent–solvent interactions, including entropy and enthalpy components, which cannot be assessed from experiment. However, most of the arguments in favour of the TATB hypothesis deal with one of these components, that is specific electrostatic solute–solvent interactions. They are inspired from the continuum Born model, according to which the excess free energy of solvation of a sphere of radius r and ionic charge Q , imbedded in a continuum of dielectric constant ϵ , is $\Delta G_{\text{Born}} = (Q^2/2r)(1/\epsilon - 1)$, and therefore *independent of the sign of Q* . According to other electrostatic models where a spherical ion interacts with a neutral solvent molecule, a charge reversal of the ion does not change the ion–dipole interaction energy, but reverses the sign of the ion–quadrupole interactions,¹¹ which are generally assumed to be negligible.^{4,5} Based on the fact that the $\text{As}\phi_4^+$ cation is somewhat larger than the $\text{B}\phi_4^-$ anion, it has been argued, based on the Born model, that the anion might be better solvated than the cation (see discussions in refs. 4 and 5). Another aspect and consequence of the TATB hypothesis concerns the interfacial behaviour of two large ions of opposite charge at a liquid–

† Non-SI units employed: 1 atm \approx 101 kPa; 1 a.u. \approx 2.63×10^6 J mol⁻¹; 1 kcal \approx 4.184 kJ.

liquid interface: if they are solvated in a similar fashion in the two adjacent liquid phases, they also should display similar properties at the interface between these two liquids, be they “alone” or in interaction.

Here we report a series of molecular dynamics (MD) simulations in explicit solvents, in relation with the TATB hypothesis. They deal with two series of model ions that are likely to meet the above criteria (i) to (vi). The first ions are tetrahedral ($\text{As}\phi_4^+$ and $\text{B}\phi_4^-$) and the second ones are spherical (S^+ and S^-). For comparison, we also consider their neutral analogues of tetrahedral ($\text{As}\phi_4^0$ and $\text{B}\phi_4^0$) and of spherical (S^0) type, where all atomic charges have been set to zero. As solvents, we consider water, chloroform and acetonitrile. Water corresponds to the reference state for free energies of transfer $\Delta G_{\text{wat} \rightarrow \text{s}}$. If the latter are the same for two ions of opposite charge, the hydration properties of these two ions should be very similar, if not identical. Chloroform and acetonitrile are “receiving phases”, of the weakly polar and polar aprotic type, respectively.

Two series of analyses are performed. The first one deals with the solvation properties of individual species. Structural features are characterized by the ion–solvent radial distribution functions (RDFs) and typical snapshots extracted from the MD trajectories. Energy component analysis is also reported with a particular focus on the electrostatic contributions of the solute–solvent interactions, and on short-range (“first shell”)/long-range contributions. Although the corresponding numbers are not physically observable quantities, they are important for our understanding of *differences* in solvent interactions when the sign of the ionic charge is reversed. Beyond single ion behaviour, we also investigate, in relation with the TATB hypothesis, the question of ion pairing between the $\text{As}\phi_4^+$ and $\text{B}\phi_4^-$ ions in the three solvents, and the interfacial behaviour of these ions at a water–chloroform interface represented explicitly. The second series of computations addresses the *differences in solvation free energies* between a given cation and the related anion in a given solvent. These simulations start with the neutral tetrahedral $\text{As}\phi_4^0$, $\text{B}\phi_4^0$ or spherical S^0 species in a given solvent, that is where the cavitation energy^{12,13} contribution of the solvation process is already paid for. Based on statistical perturbation calculations, we calculate the changes in Gibbs free energy corresponding to the electrostatic charging processes to the anion (ΔG^{0-}) and to the cation (ΔG^{0+}). According to the TATB hypothesis, these two quantities, which involve enthalpic and entropic components, should be *equal* and *independent of the solvent*. We find that this is far from being the case. The calculations also allow to predict differences in free energies of transfer of a given cation/anion from water to a given solvent. From a computational point-of-view, a number of important issues are also addressed and four models of $\text{As}\phi_4^+$ and $\text{B}\phi_4^-$ are compared.

Methods

We used the modified AMBER4.1 software¹⁴ with the following representation of the potential energy:

$$U = \sum_{\text{bonds}} K_r(r - r_{\text{eq}})^2 + \sum_{\text{angles}} K_\theta(\theta - \theta_{\text{eq}})^2 + \sum_{\text{dihedrals}} \sum_n V_n(1 + \cos n\phi) + \sum_{i < j} \left[\frac{q_i q_j}{R_{ij}} - 2\epsilon_{ij} \left(\frac{R_{ij}^*}{R_{ij}} \right)^6 + \epsilon_{ij} \left(\frac{R_{ij}^*}{R_{ij}} \right)^{12} \right]$$

The geometries of the $\text{As}\phi_4^+$ and $\text{B}\phi_4^-$ ions (see Fig. 1) were taken from a statistical analysis of 479 $\text{As}\phi_4^+$ and 1073 $\text{B}\phi_4^-$ ions in the Cambridge crystallographic data base. The average B–C distance (1.66 Å) is somewhat shorter than the As–C distance (1.91 Å). The parameters used to calculate U come

Table 1 Charge distributions in $\text{As}\phi_4^+$ and $\text{B}\phi_4^-$. See Fig. 1 for atom definitions

| | $\text{As}\phi_4^+$ | | | | $\text{B}\phi_4^-$ |
|-------|---------------------|--------------------|--------------------|--------------------|--------------------|
| | ESP ^a | set-1 ^b | set-2 ^b | set-3 ^b | ESP ^a |
| As/B | 0.76 | 0.5 | 1.0 | 0.024 | −0.48 |
| C1/C5 | −0.12 | 0.0113 | 0.0 | 0.022 | −0.29 |
| C2/C4 | −0.16 | 0.0113 | 0.0 | 0.022 | −0.15 |
| C3 | −0.07 | 0.0114 | 0.0 | 0.022 | −0.24 |
| C6 | −0.12 | 0.0114 | 0.0 | 0.022 | 0.30 |
| H1/H5 | 0.15 | 0.0114 | 0.0 | 0.022 | 0.14 |
| H2/H4 | 0.18 | 0.0114 | 0.0 | 0.023 | 0.13 |
| H3 | 0.15 | 0.0114 | 0.0 | 0.022 | 0.15 |

^a Charges obtained from a 3-21G basis set. ^b In these models, the atomic charges of $\text{As}\phi_4^+$ and $\text{B}\phi_4^-$ are identical but of opposite sign.

from the AMBER force field,¹⁵ allowing for internal ion flexibility and dynamics. The atomic charges used throughout the whole study were derived from *ab initio* 3-21G electrostatic potentials (“ESP charges”; Table 1). Additional tests were performed with three other electrostatic models (set-1 to set-3; Table 1). In set-1, the charge of the central As/B atom is +0.5/−0.5 e and the remaining charge is equally spread over all other atoms. In set-2, the total +/−1 charge sits on the central atom, while all others are neutral. In set-3, the charge is equally diluted on all atoms, including the central one. In the neutral analogues $\text{As}\phi_4^0$ and $\text{B}\phi_4^0$ all atoms have a zero charge. The torsion potentials V_i for the As–C bond of $\text{As}\phi_4^+$ and the B–C bond of $\text{B}\phi_4^-$ were set to zero. The water, acetonitrile and chloroform solvents were represented explicitly with the TIP3P¹⁶, OPLS and OPLS¹⁷ models, respectively. Other models of chloroform were also tested. In the “standard calculations” the non-bonded interactions were calculated with a residue-based cutoff of 11 Å in water, 13 Å in acetonitrile and 15 Å in chloroform. Other test calculations were performed using larger cutoff distances. The solutes were immersed at the center of cubic boxes of pure solvents or at the interface between two adjacent boxes of pure chloroform and water (Fig. 2 and Table 2), represented with periodic boundary conditions in the three directions.

The MD simulations were performed at 300 K, at $P = 1$ atm. All C–H, O–H, H···H, C–Cl and Cl···Cl “bonds”

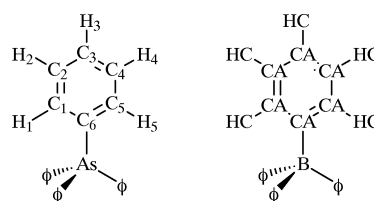


Fig. 1 Definition of atom labels (left) and atom types (right) used in both $\text{As}\phi_4^+$ and $\text{B}\phi_4^-$ ions.

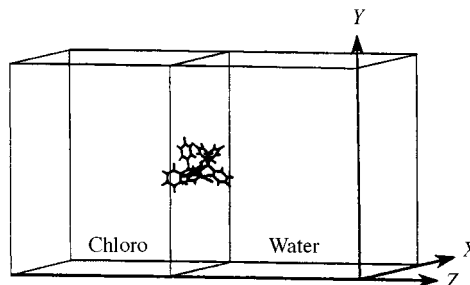


Fig. 2 Representation of an $\text{As}\phi_4^+\text{B}\phi_4^-$ ion pair at a water–chloroform interface.

Table 2 Simulation conditions in water, chloroform, acetonitrile and at the water–chloroform interface

| Solute | Solvent | Box size/Å ³ | Number of solvent molecules | Time/ps | Cut off/Å |
|---|---------------|-----------------------------|-----------------------------|---------|-----------|
| AsΦ ₄ ⁺ , BΦ ₄ [−] | Acetonitrile | 35 × 36 × 36 | 505 | 200 | 13 |
| AsΦ ₄ ⁺ , BΦ ₄ [−] ^a | Chloroform | 37 × 38 × 38 | 390 | 200 | 15 |
| AsΦ ₄ ⁺ , BΦ ₄ [−] | Polar chloro. | 37 × 38 × 38 | 390 | 200 | 15 |
| AsΦ ₄ ⁺ , BΦ ₄ [−] ^a | Water | 29 × 30 × 30 | 873 | 200 | 11 |
| AsΦ ₄ BΦ ₄ pair ^b | Acetonitrile | 48 × 37 × 36 | 709 | 600 | 13 |
| | Chloroform | 50 × 39 × 38 | 543 | 600 | 15 |
| | Water | 42 × 30 × 31 | 1279 | 600 | 11 |
| AsΦ ₄ ⁺ AsΦ ₄ ⁺ pair | Chloroform | 43 × 38 × 37 | 450 | 200 | 15 |
| | Water | 38 × 38 × 38 | 1860 | 200 | 11 |
| BΦ ₄ [−] BΦ ₄ [−] pair | Chloroform | 44 × 38 × 38 | 476 | 200 | 15 |
| | Water | 38 × 37 × 37 | 1723 | 200 | 11 |
| AsΦ ₄ ⁺ , BΦ ₄ [−] ^b | Interface | | 260 chloro | | 12 |
| | water–chloro. | 32 ² × (34 + 28) | 962 water | 1000 | |
| AsΦ ₄ BΦ ₄ pair ^b | Interface | | 264 chloro | | 12 |
| | water–chloro. | 38 ² × (34 + 28) | 1333 water | 1000 | |
| S ⁺ , S ⁰ , S [−] | Acetonitrile | 36 × 36 × 35 | 501 | 200 | 13 |
| | Chloroform | 38 × 38 × 37 | 389 | 200 | 15 |
| | Water | 30 × 30 × 29 | 871 | 200 | 11 |

^a The same conditions have been used for AsΦ₄⁺, BΦ₄[−], AsΦ₄[−], BΦ₄⁺ and neutral AsΦ₄⁰, BΦ₄⁰ species. ^b The same conditions have been used for AsΦ₄⁺, BΦ₄[−] and neutral AsΦ₄⁰, BΦ₄⁰ species.

were constrained with SHAKE, using a timestep of 1 fs. After 1000 steps of energy minimization, 5 ps of MD were first performed with the solute kept frozen. This was followed by 200 to 1000 ps of free MD (see Table 2).

Free energy calculations

The difference in free energies of solvation between states A and B was calculated using the statistical perturbation FEP theory and the windowing technique,¹⁴ with

$$\Delta G = \sum \Delta G_{\lambda}$$

and

$$\Delta G_{\lambda} = RT \log \left\langle \exp \left(\frac{U_{\lambda} - U_{\lambda+\Delta\lambda}}{RT} \right) \right\rangle_{\lambda}$$

The potential energy U_{λ} was calculated using a linear combination of charges and parameters of the initial state ($\lambda = 1$) and final state ($\lambda = 0$): $q_{\lambda} = \lambda \cdot q_1 + (1 - \lambda) \cdot q_0$. The number of windows is given in Table 6 and in Section 7. In each window, 2 ps of equilibration were followed by 3 ps of data collection and the change of free energy ΔG was averaged from the forward and backward cumulated values.

Analysis of results

Average structures, radial distribution functions (RDFs), solute–solvent (E_{sx}) and solvent–solvent (E_{ss}) interaction energies and their electrostatic/van der Waals components were calculated from the trajectories saved every 0.5 ps. For the simulations at the interface, the position of the interface was recalculated at each step, and defined as the intersection between the density curves of the water and chloroform liquids.

Results

The results are presented as follows. In Section 1, we describe the charge distribution used to model the AsΦ₄⁺ and BΦ₄[−] ions. This is followed by the solvation characteristics of these ions, compared to tetrahedral analogues in water, chloroform and acetonitrile (Section 2), and by results concerning the question of ion pairing in solution (Section 3). In Section 4, the solvation of spherical S⁺ and S[−] ions is described in the three solvents. Section 5 deals with the interfacial properties of

AsΦ₄⁺ and BΦ₄[−] at the water–chloroform interface. The question of relative free energies of solvation of AsΦ₄⁺ and BΦ₄[−], obtained from charging their neutral analogues AsΦ₄⁰ and BΦ₄⁰, is described in Section 6. These results are contrasted with those corresponding to the electrostatic charging of a neutral sphere S⁰ to S⁺ and to S[−]. We finally consider the question of differences in free energies of transfer from water to the organic solvents (Section 7).

1 Charge distribution in the AsΦ₄⁺ and BΦ₄[−] ions

In principle, in the context of the TATB hypothesis, the precise charge distribution should be of little importance, provided that the ions have “a similar and inert periphery”. There is no unique atomic charge distribution for a given molecular solute, as the atomic charges have no physical meaning and depend on the method of derivation. There is also no firm criteria to provide a balanced description of first row (B, C, H)/third row (As) atoms. Our choice was to fit ESP potentials, following a methodology widely used for polar solutes,¹⁸ using a 3-21G basis fitted consistently for the As, B, C and H atoms. Table 1 shows that the central atom bears most of the total charge (As^{+0.76}; B^{−0.48}), while the remaining charge is spread on the aromatic groups. In both ions, the aromatic C–H bonds display a clear C^{δ−}H^{δ+} polarity, where the protons are positively charged. Thus, the charges in AsΦ₄⁺ and BΦ₄[−] are not simply reversed. It can be noticed that the HOMO is of negative energy (−0.17 a.u.), that is, the anion is correctly described by a bound state. In addition, with these ESP charges, the AsΦ₄⁺ and BΦ₄[−] ions have a similar C^{δ−}H^{δ+} periphery. All simulations on AsΦ₄⁺ and BΦ₄[−] were performed with this set of charges. In addition, three other models (set-1 to set-3) were tested for the free energy calculations.

2 The AsΦ₄⁺ and BΦ₄[−] ions and their (hypothetical) tetrahedral analogues (BΦ₄⁺, AsΦ₄[−], AsΦ₄⁰ and BΦ₄⁰) in pure water, chloroform and acetonitrile solutions

In solution, the AsΦ₄⁺ and BΦ₄[−] ions are not rigid, but undergo coupled rotations of the their phenyl rings (“gearing effect”) that lead to the average time equivalence of all *ortho* and *meta* protons, in agreement with NMR data. The two ions display very different interaction energies E_{sx} with water, with acetonitrile, as well as with chloroform (Table 3). The

Table 3 The $\text{As}\phi_4^+$ and $\text{B}\phi_4^-$ ions and their analogues simulated in pure water, chloroform and acetonitrile liquids. Average solute–solvent E_{sx} and solvent–solvent E_{ss} interaction energies (kcal mol^{-1}) calculated between 50–200 ps

| Solute | $\text{As}\phi_4^+$ | $\text{B}\phi_4^-$ | $\text{As}\phi_4^0$ | $\text{B}\phi_4^0$ | $\text{As}\phi_4^-$ | $\text{B}\phi_4^+$ | $\text{As}\phi_4^{+e}$ | $\text{B}\phi_4^{-f}$ |
|-------------------------|---------------------|--------------------|---------------------|--------------------|---------------------|--------------------|------------------------|-----------------------|
| Water | | | | | | | | |
| $E_{\text{sx total}}^a$ | –85 | –121 | –33 | –32 | –79 | –115 | –84 | –118 |
| $E_{\text{sx elec}}^a$ | –53 | –93 | 0 | 0 | –49 | –83 | –53 | –88 |
| $E_{\text{ss total}}^b$ | –6934 | –6886 | –7023 | –6939 | –6899 | –6906 | –6936 | –6910 |
| $E_{\text{ss elec}}^b$ | –8131 | –8074 | –8250 | –8133 | –8097 | –8097 | –8130 | –8106 |
| Chloroform | | | | | | | | |
| $E_{\text{sx total}}^a$ | –65 | –87 | –46 | –45 | –76 | –65 | +62 | –97 |
| $E_{\text{sx elec}}^a$ | –15 | –38 | 0 | 0 | –28 | –18 | –16 | –38 |
| $E_{\text{ss total}}^c$ | –1979 | –1977 | –1997 | –1979 | –1985 | –1972 | –1981 | –1985 |
| $E_{\text{ss elec}}^c$ | –49 | –45 | –53 | –51 | –47 | –47 | –48 | –47 |
| Acetonitrile | | | | | | | | |
| $E_{\text{sx total}}^a$ | –94 | –101 | –47 | –45 | — | — | — | — |
| $E_{\text{sx elec}}^a$ | –46 | –58 | 0 | 0 | — | — | — | — |
| $E_{\text{ss total}}^d$ | –2557 | –2555 | –2595 | –2578 | — | — | — | — |
| $E_{\text{ss elec}}^d$ | –950 | –947 | –976 | –970 | — | — | — | — |

^{a–d} Fluctuations are about (a) 80, (b) 30, (c) 20, (d) 6–7 kcal mol^{-1} . ^e Calculations performed on $\text{As}\phi_4^+$ with an As–C distance of 1.66 Å, instead of 1.91 Å. ^f Calculations performed on $\text{B}\phi_4^-$ with a B–C distance of 1.91 Å, instead of 1.66 Å.

anion interacts more than the cation with the three solvents ($\Delta E_{\text{sx}} = 36, 7$, and 22 kcal mol^{-1} , respectively), mostly due to the differences in the electrostatic components ($\Delta E_{\text{sx elec}} = 40, 12$ and 23 kcal mol^{-1} , respectively). We notice that the latter do not follow the order of solvent polarities (water > acetonitrile > chloroform). Some specific solvation features are analyzed below, with a particular focus on first-shell solvent molecules, which clearly determine the observed trends.

We first consider the aqueous solution. Table 3 shows that the better hydration of $\text{B}\phi_4^-$ is not due to the somewhat smaller size of the anion. Indeed, a lengthening of the B–C bond from 1.66 to 1.91 Å decreases the interaction of $\text{B}\phi_4^-$ with water by 3 kcal mol^{-1} , while a shortening the As–C bond of $\text{As}\phi_4^+$ to 1.66 Å decreases this interaction by 1 kcal mol^{-1} only. As a result, the “stretched” $\text{B}\phi_4^-$ anion still interacts much more with water than the “shortened” $\text{As}\phi_4^+$ cation ($\Delta E_{\text{sx}} = 34 \text{ kcal mol}^{-1}$), again due to electrostatics.

The radial distribution functions (RDFs) and snapshots in water (Fig. 3) provide a structural basis for the better hydration of $\text{B}\phi_4^-$. The first-shell water molecules of $\text{As}\phi_4^+$ display similar average $\text{H}_w \cdots \text{As}$ and $\text{O}_w \cdots \text{As}$ distances, as their

O–H dipoles point to the centre of the carbon rings, forming $\text{O} \cdots \text{H} \cdots \pi$ interactions. Thus, these water molecules do not display an optimal orientation with respect to $\text{As}^{\delta+}$. Such an orientation would disrupt the $\text{O} \cdots \text{H} \cdots \pi$ “bonds”. The first hydration shell of $\text{B}\phi_4^-$ is quite different, as some water molecules can achieve *both* $\text{O} \cdots \text{H} \cdots \pi$ interactions with the phenyl rings and charge/dipole interactions with $\text{B}^{\delta-}$. As a result, their water protons H_w are closer to $\text{B}^{\delta-}$ than the O_w atoms (Fig. 3). Some water molecules achieve bridging $\pi \cdots \text{HOH} \cdots \pi$ interactions over two phenyl rings, while others achieve one $\text{OH} \cdots \pi$ interaction only (Fig. 3). Within 4.0 Å from the central atom, there are 3.9 H_w and 0.2 O_w around $\text{B}\phi_4^-$, whereas there are no water atoms around $\text{As}\phi_4^+$. An energy component analysis, taking into account only those water molecules that are within 7 Å from the central atom (Table 4) confirms their larger interactions with $\text{B}\phi_4^-$, compared to $\text{As}\phi_4^+$ (by about $41 \pm 7 \text{ kcal mol}^{-1}$). Both ions display a peak in the O_w RDFs at about 5 Å, which corresponds to the hydration of the “core”, and another broad peak at 7.5–8.0 Å, corresponding to the hydration of peripheral C–H_{para} protons.

This analysis makes clear that the sign of the ionic charge and the precise charge distribution in the ions determine their hydration properties. This conclusion is confirmed by the calculations on the hypothetical $\text{As}\phi_4^-$ and $\text{B}\phi_4^+$ ions, where all atomic ESP charges have been reversed (Table 3). Now, $\text{B}\phi_4^+$ becomes better hydrated than $\text{As}\phi_4^-$ ($\Delta E_{\text{sx}} = 35 \text{ kcal mol}^{-1}$), again due to the electrostatic component. The hydration schemes around $\text{B}\phi_4^+$ and $\text{As}\phi_4^-$ are also quite different from the ones around the corresponding (real) $\text{As}\phi_4^+$ and $\text{B}\phi_4^-$ ions.

Although chloroform is less polar than water, it also displays specific interactions with the ions. The first-shell CHCl_3 molecules interact more strongly than the remaining ones by $26 \pm 4 \text{ kcal mol}^{-1}$ (Table 4) because of their different orientations. Around $\text{B}\phi_4^-$, they point their C–H “proton” toward the $\text{B}^{\delta-}$ atom in a C_{3v} -type arrangement leading to secondary interactions between the Cl atoms of CHCl_3 and C–H aromatic protons (Fig. 4). As a result, the first $\text{B} \cdots \text{C}_{\text{chlor}}$ peak is found at a shorter distance than the $\text{B} \cdots \text{Cl}_{\text{chlor}}$ peak. Around $\text{As}\phi_4^+$, the orientation of CHCl_3 molecules is inverted: the Cl atoms are closer to As than the H atoms, and the C–H dipole points outwards, as expected from the $\text{As}^{\delta+} \cdots \text{CHCl}_3$ charge–dipole interactions. This does not lead, however, to attractive interactions with the aromatic rings and, as a result, $\text{As}\phi_4^+$ interacts less than $\text{B}\phi_4^-$ with chloroform.¹⁹

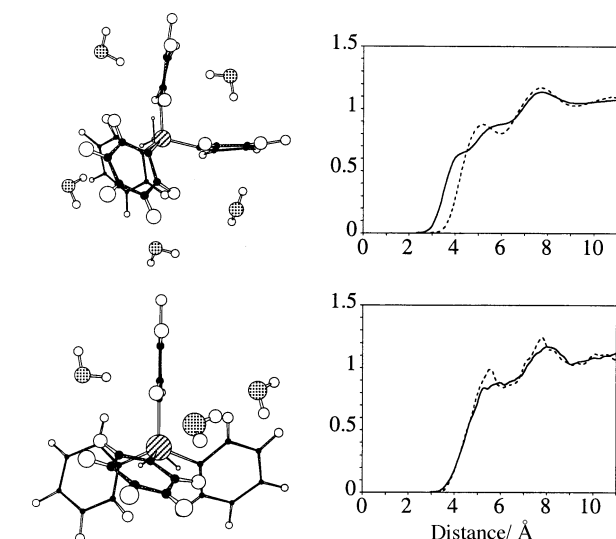


Fig. 3 The $\text{B}\phi_4^-$ (top) and $\text{As}\phi_4^+$ (bottom) ions in water. Typical snapshots and RDFs around the central atom (B or As) of O_w (dotted line) and H_w (full line).

Table 4 The $\text{As}\phi_4^+$ and $\text{B}\phi_4^-$ ions in pure water, chloroform, polar chloroform and acetonitrile liquids. Shell analysis of solute-solvent interaction energies (kcal mol^{-1}) performed between 50–200 ps. Group 1: First-shell solvent molecules [*i.e.*, which have any atom within 7 Å (in water and acetonitrile) or 8 Å (in chloroform) from the central As or B atom]. Group 2: All other solvent molecules within the cutoff distance^a

| | $\text{As}\phi_4^+$ | | | | $\text{B}\phi_4^-$ | | | |
|------------------------|---------------------|---------|---------------|---------|--------------------|---------|---------------|---------|
| | Water | Chloro. | Polar chloro. | Aceton. | Water | Chloro. | Polar chloro. | Aceton. |
| $E_{\text{sx1 elec}}$ | –22 | –5 | –7 | –15 | –70 | –26 | –27 | –32 |
| $E_{\text{sx1 total}}$ | –39 | –34 | –35 | –40 | –84 | –60 | –51 | –53 |
| $E_{\text{sx2 elec}}$ | –31 | –11 | –15 | –30 | –25 | –13 | –27 | –26 |
| $E_{\text{sx2 total}}$ | –46 | –29 | –34 | –54 | –39 | –28 | –51 | –48 |
| $E_{\text{sx elec}}$ | –53 | –16 | –22 | –46 | –95 | –39 | –54 | –58 |
| $E_{\text{sx total}}$ | –85 | –63 | –69 | –94 | –123 | –88 | –102 | –101 |

^a Fluctuations are about 3–7 kcal mol^{-1} .

In acetonitrile, the difference between the ion-solvent interaction energies is smaller than in chloroform ($\Delta E_{\text{sx}} = 7 \pm 7 \text{ kcal mol}^{-1}$). The acetonitrile molecules do not display any marked orientation preferences around the cation compared to the anion. The RDFs and typical snapshots (Fig. 5) show that, around a given ion, the two opposite orientations of the

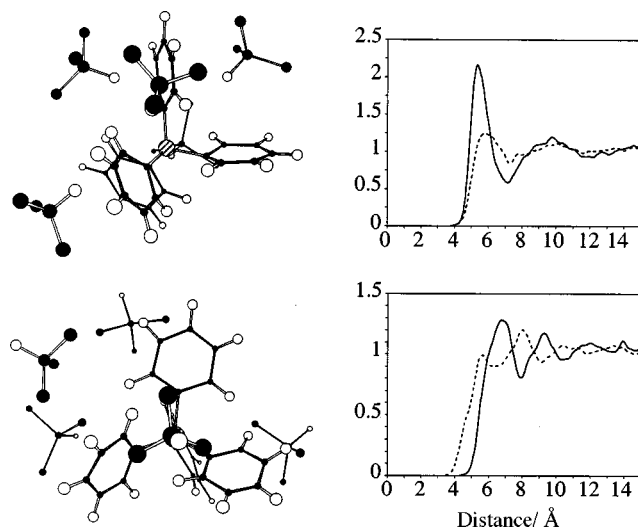


Fig. 4 The $\text{B}\phi_4^-$ (top) and $\text{As}\phi_4^+$ (bottom) ions in chloroform. Typical snapshots and RDFs around the central atom (B or As) of Cl_{chlor} (dotted line) and C_{chlor} (full line).

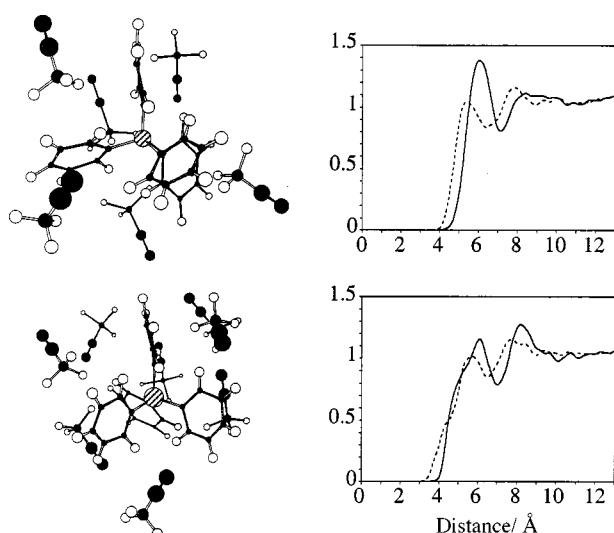


Fig. 5 The $\text{B}\phi_4^-$ (top) and $\text{As}\phi_4^+$ (bottom) ions in acetonitrile. Typical snapshots and RDFs around the central atom (B or As) and N_{acet} (dotted line) of Me_{acet} (full line).

MeCN dipoles with respect to the central atom are simultaneously present.

Generally speaking, when ion-solvent electrostatic attractions increase, the solvent-solvent E_{ss} interactions become less attractive, as the orientation of the first-shell solvent molecules with respect to the solute prevents optimal solvent-solvent interactions (Table 3). For instance, the larger interactions of water with $\text{B}\phi_4^-$, compared to $\text{As}\phi_4^+$ ($\Delta E_{\text{sx}} = 36 \pm 6 \text{ kcal mol}^{-1}$) are partly compensated by the change in water-water interactions ($\Delta E_{\text{ss}} = -48 \pm 80 \text{ kcal mol}^{-1}$). Thus, relative solvation energies cannot be obtained solely from the E_{sx} interaction energies. In addition, the statistical fluctuations on E_{ss} are quite large. Free energy calculations are required to more quantitatively account for the differences in thermodynamic aspects of the solvation (see Sections 6 and 7).

3 The $\text{As}\phi_4^+\text{B}\phi_4^-$ ion pair and its $\text{As}\phi_4^0\text{B}\phi_4^0$ analogue in pure water, chloroform and acetonitrile solutions

As in real transfer experiments the cations and anions are simultaneously present in solution, it is important to test the status of the $\text{As}\phi_4^+\text{B}\phi_4^-$ ion pair as a function of the solvent. The TATB hypothesis implicitly assumes that the solvation properties of the salt can be described by those of the individual ions, which have therefore no direct contact. In this section, we report on MD simulations performed for 600 ps, starting from an intimate ion pair in water, chloroform and acetonitrile solutions, which show that the ion pair remains intimate in the three solvents (Fig. 6): the $\text{As}\cdots\text{B}$ distance oscillates between 6.5 and 9.0 Å along the simulations. Both ions rotate and display interionic electrostatic attractions, exchanging dynamically between π - π stacking (dipole-dipole) and/or $\text{C}-\text{H}\cdots\pi$ (quadrupole-quadrupole) interactions between their phenyl rings. In water, additional stabilization comes from “hydrophobic forces”, as pointed out by simulations of the $\text{As}\phi_4^0\text{B}\phi_4^0$ pair of the uncharged analogues (Fig. 6). This pair remains intimate in water, at nearly the same $\text{As}\cdots\text{B}$ distance as in the charged pair (6.5 Å), but dissociates rapidly in chloroform and acetonitrile solutions. We thus conclude that the solvation of a given $\text{As}\phi_4^+$ or $\text{B}\phi_4^-$ ion may depend on its counter ion.

As it has been suggested that π -delocalized cations might display mutual attractions in solution^{20,21} or in the solid state,^{22,23} we also investigated the $\text{As}\phi_4^+\text{As}\phi_4^+$ and $\text{B}\phi_4^-\text{B}\phi_4^-$ like ion pairs. They were found to dissociate in the three solvents (Fig. 7).

4 Solvation of the spherical S^+ , S^- and S^0 species in water, chloroform and in acetonitrile solutions

The importance of the positive/negative charge of the solute is further demonstrated by MD simulations performed on a large sphere in its neutral (S^0) and charged states (S^+ and S^-). These solutes are represented by van der Waals parameters $R^* = 5.5 \text{ Å}$ (close to the average radius of gyration of the

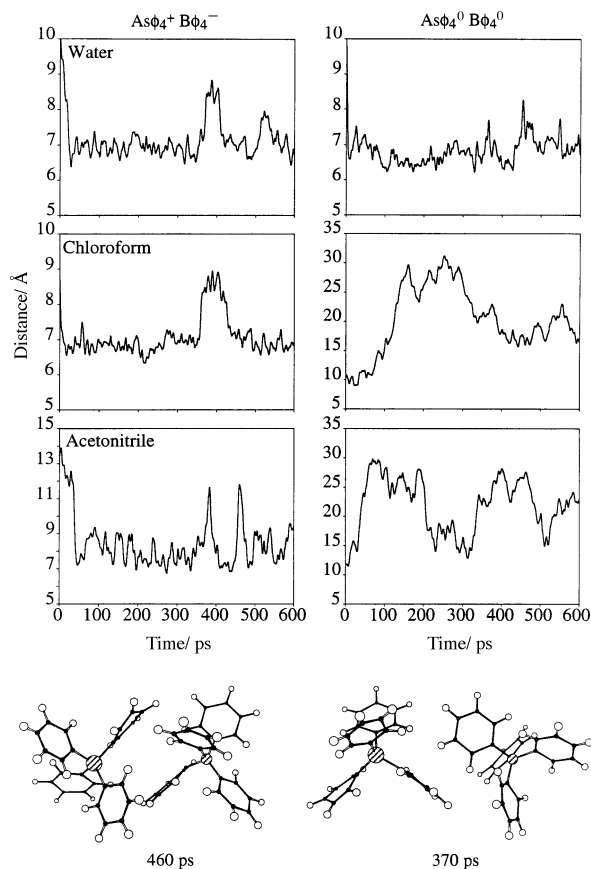


Fig. 6 The $\text{As}\Phi_4^+\text{B}\Phi_4^-$ ion pair and its analogue $\text{As}\Phi_4^0\text{B}\Phi_4^0$. From top to bottom: simulations in water, in chloroform and in acetonitrile. $\text{As}\cdots\text{B}$ distance as a function of time (ps). Bottom: snapshots of the ion pair in water at a $\text{As}\cdots\text{B}$ separation of 7.4 Å (at 460 ps) and of 9 Å (at 370 ps).

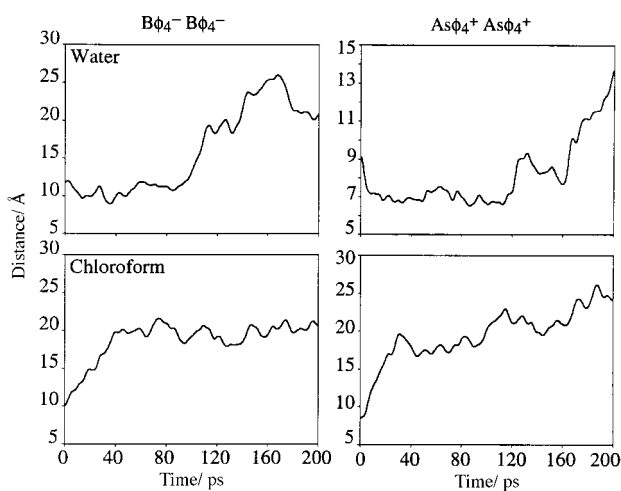


Fig. 7 The $\text{B}\Phi_4^-\text{B}\Phi_4^-$ and $\text{As}\Phi_4^+\text{As}\Phi_4^+$ ion pairs in water (top) and in chloroform (bottom). $\text{B}\cdots\text{B}$ and $\text{As}\cdots\text{As}$ distances as a function of time.

Table 5 Spherical S^0 , S^+ and S^- species in water, chloroform and acetonitrile solutions. Average solute–solvent (E_{sx}) and solvent–solute (E_{ss}) interaction energies (kcal mol^{-1}) calculated between 50–200 ps

| | Water | | | Chloroform | | | Acetonitrile | | |
|-------------------------|--------------|--------------|--------------|--------------|--------------|--------------|--------------|--------------|--------------|
| | S^0 | S^+ | S^- | S^0 | S^+ | S^- | S^0 | S^+ | S^- |
| $E_{\text{sx elec}}^a$ | 0 | –51 | –39 | 0 | –9 | –20 | 0 | –37 | –33 |
| $E_{\text{ss total}}^a$ | –6 | –55 | –42 | –8 | –17 | –27 | –6 | –40 | –36 |
| $E_{\text{ss elec}}^b$ | –8098 | –8061 | –8037 | –44 | –43 | –40 | –948 | –932 | –933 |
| $E_{\text{ss total}}^b$ | –6911 | –6882 | –6869 | –1248 | –1240 | –1240 | –2478 | –2464 | –2465 |

^{a,b} Fluctuations are around (a) 5 and (b) 30 kcal mol^{-1} .

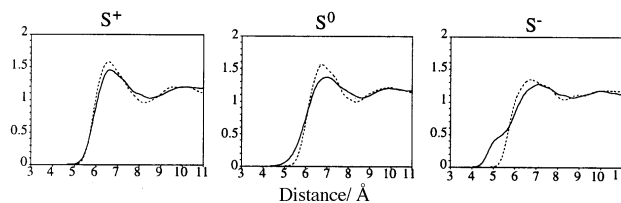


Fig. 8 Spherical S^+ , S^0 and S^- species in water: O_w (dotted line) and H_w (full line) RDFs around the centre of S.

$\text{As}\Phi_4^+$ and $\text{B}\Phi_4^-$ ions, and $\epsilon = 0.1 \text{ kcal mol}^{-1}$ (close to the ϵ value of interacting solvent atoms). They meet the above mentioned criteria (i) to (vi) for the TATB hypothesis, but display marked differences in solvation properties, especially in water.

In water, the S^+ cation is found to be better hydrated than the S^- anion (Table 5) because of two cooperative features: S^+ interacts more than S^- with water ($\Delta E_{\text{sx}} = 13 \pm 4 \text{ kcal mol}^{-1}$), and the water–water interactions are more attractive around S^+ than around S^- ($\Delta E_{\text{ss}} = 13 \pm 30 \text{ kcal mol}^{-1}$, again mostly due to electrostatics). This large effect is related to the different orientations of water dipoles around the spheres. The RDFs show that solvation around S^+ or S^0 is of the “hydrophobic type”, where the O–H bonds are more or less tangential to the solute (Fig. 8): the $\text{S}\cdots\text{O}_w$ and $\text{S}\cdots\text{H}_w$ RDFs are similar below 7 Å. As the O_w charge is twice the H_w charge, this structure clearly favours interactions with a positively charged solute, as observed in clathrate-type structures of water around quaternary ammonium ions.^{24–28} This contrasts with the hydration of S^- , where some of the H_w s make closer contacts with S^- than do the O_w atoms. Additional analysis of the first solvation shells of S^0 , S^+ and S^- confirms the different orientations of water dipoles, as sketched in Fig. 9. The average SOD angle is about 110° in S^+ , 90° in S^0 and 60° in S^- . As a result, the first-shell water molecules display hydrogen bonding attractions around S^+ and repulsions around S^- . We also notice that hydration of S^0 is similar to that of S^+ , but differs from that of S^- . This analysis makes clear why S^+ is better hydrated than S^- , in contrast to $\text{As}\Phi_4^+$, which interacts less with water than $\text{B}\Phi_4^-$.

In chloroform, the trends are reversed compared to water: S^+ interacts less than S^- with the solvent ($\Delta E_{\text{sx}} = 10 \text{ kcal mol}^{-1}$), due to the electrostatic component (Table 5).

In acetonitrile solution, there is no marked difference between the interaction energies E_{sx} of S^+ vs. S^- and the solvent ($\Delta E_{\text{sx}} = 4 \pm 5 \text{ kcal mol}^{-1}$) nor between the solvent–solvent E_{ss} energies, which are nearly identical (Table 5). The RDFs do not reveal any clear structure of acetonitrile around S^0 , S^+ or S^- . Thus, again, the role of positive/negative ionic charge markedly depends on the nature of the solvent. Discrimination between the model spherical S^+ and S^- species, which meet the criteria for the reference electrolyte hypothesis, is largest in water.

5 The $\text{As}\Phi_4^+$ and $\text{B}\Phi_4^-$ ions and their analogues at the water–chloroform interface

The simulations of the isolated ions, as well as of the $\text{As}\Phi_4^+-\text{B}\Phi_4^-$ ion pairs, initially set at a water–chloroform interface,

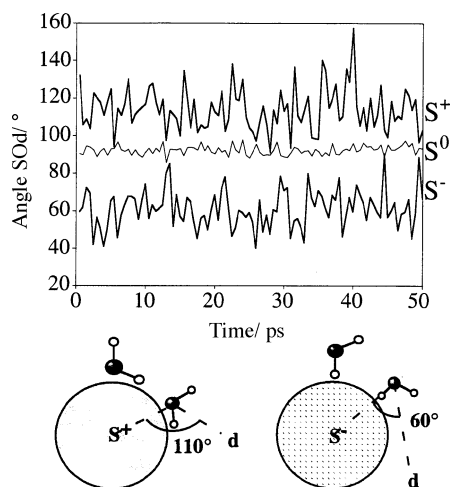


Fig. 9 Spherical S^+ , S^0 and S^- in water. Angle SOd with the first-shell molecules as a function of time. The selected water molecules have their O_w atom within 6 Å (for S^+ and S^-) or 8 Å (for S^0) from the centre of the sphere.

also reveal that the two ions interact differently with the two solvents. This is illustrated by the distances between the As and B atoms and the interface during the simulations and the snapshots of the final positions (Fig. 10).

Both ions, whose central atom is initially right at the interface, rapidly move to the chloroform phase (Fig. 10). Despite their charge, they do not migrate into water because of the higher cavitation energy (energy cost for creating a cavity¹³) of water, compared to chloroform, in relation with the differences of their surface tensions (72 and 27 mN m⁻¹, respectively).²⁹ $B\phi_4^-$ oscillates a few Angströms apart from the interface, while $As\phi_4^+$ moves deeper into chloroform (up to 6 Å). As a result, the anion is more attracted by water than the cation (by about 50 ± 6 kcal mol⁻¹ during the last 500 ps), while the difference in interaction energies with chloroform is less (8 ± 6 kcal mol⁻¹).

The importance of electrostatic forces on the interfacial behaviour is demonstrated by simulations on the neutral analogues $As\phi_4^0$ and $B\phi_4^0$, which both migrate into chloroform (at

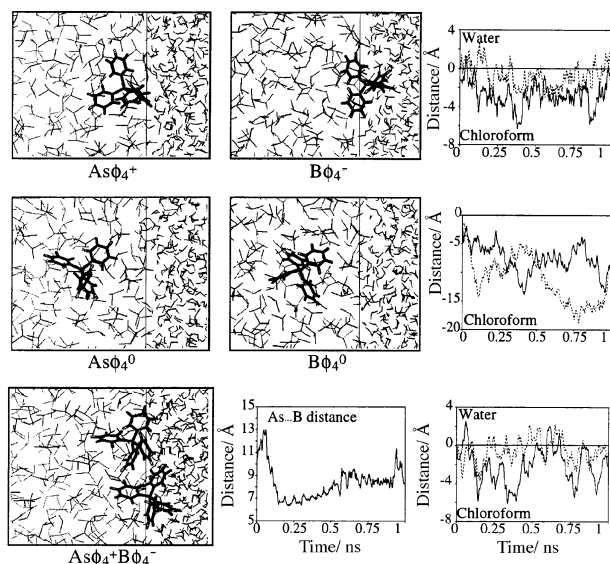


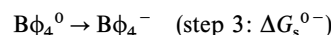
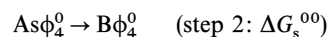
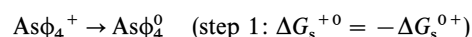
Fig. 10 Snapshots of the $As\phi_4^+$ and $B\phi_4^-$ ions (top), of their $As\phi_4^0$ and $B\phi_4^0$ neutral analogues (middle) and the $As\phi_4^+B\phi_4^-$ pair (bottom) at the water–chloroform interface after 1 ns. Right: distances between the interface and the B (dotted line) or As (full line) atoms as a function of time (ns). Bottom centre: As...B distance as a function of time (ns).

about 8 Å after 400 ps), without retaining any contact with the water phase (Fig. 10).

When the $As\phi_4^+B\phi_4^-$ pair is simulated at the interface, starting with an ionic separation of about 11 Å, the two ions collapse to form an intimate ion pair, although less tight than in pure water (the B...As distance ranges from 6.5 to 8 Å). As a result, both ions remain close to the interface, but $As\phi_4^+$ sits somewhat deeper than $B\phi_4^-$ in chloroform (Fig. 10). Thus, the anion is more surface active than the cation. Concerning the S^+ and S^- ions, the interfacial behaviour is expected to be opposite that of the tetrahedral ions, as the S^+ cation interacts better with water than S^- .

6 Differences in free energies of solvation of tetrahedral $As\phi_4^+/B\phi_4^-$ and of spherical S^+/S^- species in water, chloroform and acetonitrile solutions

In this section, we address the question of relative free energies of solvation by FEP computations where the cation is mutated stepwise into the anion (or *vice versa*), via an “alchemical route”.^{30,31} In the case of the tetrahedral ions, we decomposed the $As\phi_4^+$ to $B\phi_4^-$ mutation via the non-physical intermediate neutral states:



In a given solvent s , $\Delta G_s^{+-} = \Delta G_s^{+0} + \Delta G_s^{00} + \Delta G_s^{0-}$. According to the TATB hypothesis, ΔG_s^{+-} should be zero in any solvent. Table 6 shows that this is not the case, whatever the model of ions and the simulation conditions are. We first notice (Table 6) that the ΔG_s^{00} contribution is negative, as expected from the Born or cavitation models,^{12,13,32} but quite small and negligible (from -0.1 to -0.5 kcal mol⁻¹), compared to the two other terms. Thus, the difference in solvation free energies mostly results from the ΔG_s^{0-} and ΔG_s^{0+} contributions, which are negative and different from each other. In the following, we consider the values obtained with the largest cutoff distances. However, the observed trends are independent of the cutoff (Table 6).

Among the tetrahedral ions, $B\phi_4^-$ is better solvated than $As\phi_4^+$ as ΔG^{0-} is more negative than ΔG^{0+} in water (-41 and -31 kcal mol⁻¹, respectively), in chloroform (-22 and -8 kcal mol⁻¹, respectively) and acetonitrile (-27 and -23 kcal mol⁻¹, respectively).

In the case of isovolumic spherical ions, the ΔG_s^{00} contribution is zero. These ions behave opposite to the tetrahedral ones, and display nonzero values of ΔG^{+-} that are spectacularly solvent dependent. This value is largest and positive in water (15.9 kcal mol⁻¹), negative in chloroform (-4.8 kcal mol⁻¹), and nearly zero in acetonitrile. Indeed, in water, charging S^0 to S^+ ($\Delta G_{\text{wat}}^{0+}$) is far more favourable (more than twice) than charging S^0 to S^- ($\Delta G_{\text{wat}}^{0-}$).³³ As pointed out in Section 4, this stems from the fact that the water structure around S^0 is “preorganized” for complexing a S^+ species, as it creates a negative potential (-9.5 ± 2 kcal mol⁻¹) at the centre of the sphere. In addition, charging S^0 to S^+ can be performed without markedly disrupting the water structure, while charging S^0 to S^- involves the rupture of first-shell hydrogen-bond networks, and inversion of water dipoles. We notice that the potential created by the water molecules around the neutral $B\phi_4^0$ and $As\phi_4^0$ species is also negative (-9.5 ± 0.5 kcal mol⁻¹), and thus should favour charging to $As\phi_4^+$ compared to $B\phi_4^-$. Thus, the fact that $B\phi_4^-$ is better hydrated than $As\phi_4^+$ is due to specific interactions of water with the anion as described above, rather than to a “preorganization” of water around $B\phi_4^0$ or $As\phi_4^0$. The above

Table 6 Summary of consistent calculations of ΔG_s (kcal mol⁻¹) and differences ΔG_s^{+-} in free energies of solvation of $\text{As}\phi_4^+/\text{B}\phi_4^-$ and S^+/S^- in a given solvent *s*. The differences between forward and backward calculated ΔG_s are about 0.2 kcal mol⁻¹. Mutations were achieved in 21 windows in water and acetonitrile, and in 51 windows in chloroform. Unless otherwise specified, all values for $\text{As}\phi_4^+/\text{B}\phi_4^-$ are obtained with the ESP charges

| Solvent | Cutoff/Å | $-\Delta G_s^{0+}$ ΔG_s^{00} $-\Delta G_s^{0-}$ | | | | ΔG_s^{+-} | | $\Delta\Delta G_t^a$ |
|---------------------|-----------------|---|---------------------------------|--------------------------------|--------------------|---------------------------------|--------------------|----------------------|
| Tetrahedral species | | $\text{As}\phi_4^+ \rightarrow$ | $\text{As}\phi_4^0 \rightarrow$ | $\text{B}\phi_4^0 \rightarrow$ | $\text{B}\phi_4^-$ | $\text{As}\phi_4^+ \rightarrow$ | $\text{B}\phi_4^-$ | |
| Water | 11 | 31.5 | -0.4 | -41.1 | | -10.0 | | — |
| | 11/15 | 29.7 | -0.4 | -37.8 | | -8.5 | | — |
| | 11 ^b | 37.1 | -0.4 | -20.4 | | 16.3 ^d | | — |
| | 11 ^c | 44.4 | -0.4 | -30.3 | | 13.7 ^e | | — |
| | 11 ^d | 33.2 | -0.4 | -17.0 | | 15.8 ^f | | — |
| Chloroform | 15 ^e | 7.6 | -0.1 | -22.1 | | -14.6 | | 4.6 |
| | 15 ^f | 7.2 | -0.1 | -20.3 | | -13.2 | | 3.2 |
| | 15 ^b | 9.1 | -0.1 | -17.4 | | -8.4 ^d | | 24.7 |
| | 15 ^d | 9.1 | -0.1 | -17.3 | | -8.3 ^f | | 24.1 |
| Acetonitrile | 13 | 23.0 | -0.4 | -27.0 | | -4.4 | | -5.6 |
| Spherical species | | $\text{S}^+ \rightarrow$ | S^0 | $\rightarrow \text{S}^-$ | | $\text{S}^+ \rightarrow$ | S^- | |
| Water | 11 | 30.7 | | -13.5 | | 17.2 | | — |
| | 11/15 | 28.1 | | -12.2 | | 15.9 | | — |
| Chloroform | 15 | 7.2 | | -12.0 | | -4.8 | | 22.0 |
| Acetonitrile | 13 | 19.5 | | -18.8 | | 0.7 | | 16.5 |

^a $\Delta\Delta G_t = \Delta G_t^+ - \Delta G_t^-$ is the difference in free energies of transfer of the cation and the anion, computed consistently (see text). ^{b-d} The charges used for $\text{As}\phi_4^+$ and $\text{B}\phi_4^-$ are (b) set-1, (c) set-2 or (d) set-3 defined in Table 2. ^e OPLS model of chloroform. ^f All atom model of chloroform, from ref. 53.

analysis makes clear why “water cages” (clathrates) are generally found around large cations,^{24–28} but never, to our knowledge, around large anions. This can also be considered as an indirect proof of the importance of sign reversal in ions.

In chloroform, the S^+ and S^- spherical ions are not equally solvated, but the trend is inverted, compared to water: the anion is better solvated than the cation by about 5 kcal mol⁻¹ ($\Delta G_{\text{chlor}}^{0-} = -12.0$ kcal mol⁻¹ and $\Delta G_{\text{chlor}}^{0+} = -7.2$ kcal mol⁻¹). In acetonitrile, both S^0 to S^- and S^0 to S^+ mutations lead to identical energy changes ($\Delta G_{\text{acet}}^{0+} = \Delta G_{\text{acet}}^{0-} = -19 \pm 0.5$ kcal mol⁻¹), indicating that the solvation of these two ions is similar. This is fully consistent with the lack of significant differences in interaction energies E_{sx} reported above. Thus, a charge reversal from S^+ to S^- has minor energetic effects in acetonitrile. Comparison of tetrahedral *vs.* spherical species shows that the difference in solvation energies of a large cation *vs.* an isostructural anion depends markedly on the solvent. Effects are largest in water and smallest in acetonitrile. They thus do not simply follow the solvent polarity. These conclusions are strengthened by a number of computational tests, related to the treatment of long-range electrostatic interactions and to the sampling problem.³⁴

For the tetrahedral species, the ΔG_s depend, as stressed above, on the precise charge distributions. This is first demonstrated by charging $\text{B}\phi_4^0$ to $\text{B}\phi_4^+$ and $\text{As}\phi_4^0$ to $\text{As}\phi_4^-$ (“inversed analogues” with ESP charges). The corresponding ΔG_s (-47 and -18 kcal mol⁻¹, respectively in water; -11 and -17 kcal mol⁻¹ in chloroform) differ markedly from the values obtained for the “real ions”. However, they lead to $\Delta G_{\text{wat}}^{+-} = 30$ kcal mol⁻¹, that is, again to a marked cation/anion discrimination by the solvent. The second series of tests deals with the “hand-made” electrostatic models where the atomic charges of two ions are identical, but reversed (set-1 to set-3, defined in Table 2). In water, all three lead to a marked preference for cation hydration ($\Delta G_{\text{wat}}^{+-}$ ranges from 13.7 to 16.3 kcal mol⁻¹; see Table 6). This can be explained by the negative potential created by water at the centre of the $\text{As}\phi_4^0$ and $\text{B}\phi_4^0$ species and by the absence of specific solvation patterns with these models. The important result is that in water, $\Delta G_{\text{wat}}^{+-}$ is far from being close to zero with any of these models. In chloroform, where only set-1 and set-3 models were compared, $\Delta G_{\text{chlor}}^{+-}$ remains different from zero and negative

(about -8 kcal mol⁻¹); $\text{B}\phi_4^-$ is better solvated than $\text{As}\phi_4^+$, as with the ESP model.

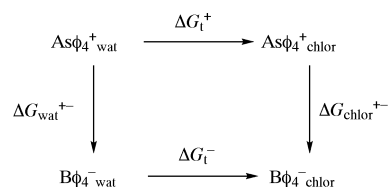
7 Differences in free energies of transfer of individual ions from water to the organic liquids

Now comes the question to more quantitatively assess the *differences* in free energies of transfer $\Delta\Delta G_t$ from water to chloroform for two ions of opposite charge. As illustrated in Scheme 1 for the $\text{As}\phi_4^+/\text{B}\phi_4^-$ pair, $\Delta\Delta G_t = \Delta G_t^+ - \Delta G_t^-$. According to this thermodynamic cycle, $\Delta\Delta G_t = \Delta G_{\text{wat}}^{+-} - \Delta G_{\text{chlor}}^{+-}$. Similarly, for the transfer to acetonitrile, $\Delta\Delta G_t = \Delta G_{\text{wat}}^{+-} - \Delta G_{\text{aceto}}^{+-}$ ($= 0$ according to the “TATB hypothesis”). In doing so, we assume that the organic phase is dry, which may not be the case as some hydrogen-bonded water molecules may follow the ion into the organic phase (“water dragging effect”).^{35,36}

For the tetrahedral ions, the results obtained with different conditions (Table 6) confirm that $\Delta G_{\text{wat}}^{+-}$ is larger than $\Delta G_{\text{chlor}}^{+-}$, implying that $\text{As}\phi_4^+$ is less easily transferred than $\text{B}\phi_4^-$ from water to chloroform. With the 15 Å cutoff, the calculated $\Delta\Delta G_t$ is quite large ($+6$ kcal mol⁻¹). The same conclusion is obtained with the ESP charges as well as with the charges of set-1 or set-3. It is confirmed using two other models of chloroform.³⁷ It seems quite paradoxical, if one considers that the anion interacts better than the cation with water, and seems therefore more “hydrophilic”.

For the transfer of $\text{As}\phi_4^+/\text{B}\phi_4^-$ to acetonitrile, the trend is opposite to the one in chloroform: $\Delta G_{\text{wat}}^{+-} - \Delta G_{\text{aceto}}^{+-}$ is negative (from -4.1 to -5.6 kcal mol⁻¹, depending on the simulation conditions), which means that the transfer of $\text{As}\phi_4^+$ to acetonitrile is preferred.

Concerning the spherical ions S^+ and S^- , which best fit the “TATB hypothesis” we calculate again a marked difference in



Scheme 1

transfer properties: S^- is more easily transferred to acetonitrile ($\Delta G_{\text{wat}}^{+-} - \Delta G_{\text{aceto}}^{+-}$ ranges from 15 to 17 kcal mol⁻¹), as well as to chloroform ($\Delta G_{\text{wat}}^{+-} - \Delta G_{\text{chlor}}^{+-} = 20.6$ kcal mol⁻¹) than S^+ . We notice that these numbers are quite large, due mostly to the better hydration of S^+ , compared to S^- .

Discussion and conclusion

MD and FEP simulations on $\text{As}\phi_4^+$ and $\text{B}\phi_4^-$ ions and analogues show that sign reversal of the ionic charge leads to marked differences in solvation properties in pure water, acetonitrile, chloroform solutions and at the water–chloroform interface. It appears clearly that, although both tetrahedral ions are similar in size and shape, $\text{As}\phi_4^+$ interacts less than $\text{B}\phi_4^-$ with all solvents. The effect of ion size is nearly negligible. In the case of the model large spherical S^+/S^- ions of identical size, which best fit the criteria for the TATB hypothesis, marked differences are also found in solvation properties and the discrimination is largest in water, where S^+ is better hydrated than S^- . Effects of charge reversal are mostly ascribable to short-range specific interactions, determined by the sign of the ionic charge, the shape of the “large ion” and the nature of the solvent.

The effect of charge reversal cannot be therefore simply assessed by solvent continuum models. Our analysis points out the role of solvent granularity of specific interactions in the first solvation shells. In the case of $\text{B}\phi_4^-$, recent spectroscopy studies of the HDO water molecules surrounding $\text{B}\phi_4^-$ and the $\text{P}\phi_4^+$ analogue of $\text{As}\phi_4^+$ in aqueous solution have been reported.³⁸ They revealed distinct differences in their hydration and concluded that the anion interacts more with water than the cation and that “the effect of $\text{B}\phi_4^-$ is determined by the anion–water interactions, while the effect of $\text{P}\phi_4^+$ is determined by water–water interactions around the cation”.³⁸ This is consistent with our results. Based on the environment analysis of $\text{B}\phi_4^-$ in solid state structures, Marcus quoted that “the energetic effect of hydrogen bonding between the uncharged water solvent molecules and this anion should not be significant”.¹⁰ This is not supported by these results. We performed a systematic search of water around the $\text{B}\phi_4^-$ and $\text{As}\phi_4^+$ ions in the Cambridge crystallographic data base. It is remarkable that the hydration patterns we calculate around $\text{B}\phi_4^-$ are identical to those found in several X-ray structures^{39,40} in which the HOH molecules display bridging $\pi \cdots \text{H}-\text{O}-\text{H} \cdots \pi$ interactions as depicted in Fig. 3. Such patterns are consistent with the IR spectroscopic results of ref. 38. They contrast with the lack of specific interactions between $\text{As}\phi_4^+$ and water in the solid state.

There are many factors that contribute to the solvation thermodynamics of ions (see discussions in refs. 10, 41 and 42 for experimental aspects and in refs. 43–47 for computational aspects). The effect of the sign of the charge is not clear. Luzhkov and Warshel compared the hydration energies of the $\text{P}\phi_4^+$ and $\text{B}\phi_4^-$ ions, using two microscopic models, where the solvent is represented either by polarizable Langevin dipoles or by explicit solvent molecules interacting with the solutes.⁴⁸ They concluded that $\text{B}\phi_4^-$ is better hydrated than $\text{P}\phi_4^+$, due to the differences in charge distribution and to “steric factors”. This is fully consistent with our results. In the case of small spherical ions (e.g., Cl^-/Cl^+), RISM-HNC calculations suggest that cations are less hydrated than the anions, due to differences in their “effective size”. Other simulations of these Cl^-/Cl^+ species at a water–dichloroethane interface suggest that Cl^- can approach closer to the interface than “ Cl^+ ” and is therefore somewhat less surface active.⁴⁹ The surface activity is generally related to the amphiphilic character of the solute and it is not clear whether Cl^- would be more “hydrophilic” than “ Cl^+ ”. Our calculations suggest that $\text{B}\phi_4^-$ is more surface active than $\text{As}\phi_4^+$, which is in

agreement with related experiments,⁵⁰ while S^+ would more surface active than S^- .

According to the TATB hypothesis, the $\text{As}\phi_4^+$ and $\text{B}\phi_4^-$ ions, or (better) the (hypothetical) S^+ and S^- ions, should display the same energies of transfer from water to any other solvent. This is not found in our simulations. With none of the models are the free energies of solvation identical. There is no simple relationship between solvent polarity and differences in solvation energies. Based on electrochemical measurements across the water–1,2-dichloroethane interface, it was found that $\text{As}\phi_4^+$ is more easily transferred than $\text{B}\phi_4^-$ (the corresponding standard Gibbs energies are -9.6 and -8.6 kcal mol⁻¹, respectively).⁵¹ However, these data may not strictly relate to our calculations, as the organic phase is different, and likely not dry. The effect of counter ion, not addressed in our FEP studies, also requires further investigations, as the nature of the $X^-\text{As}\phi_4^+$ and of $Y^+\text{B}\phi_4^-$ ion pairs may depend on the nature of the X^- and Y^+ counter ions as well as on the solvent, as suggested by our computations on the $\text{As}\phi_4^+\text{B}\phi_4^-$ pair. It is worth pointing out that the very low solubility of $\text{As}\phi_4\text{B}\phi_4$ in water (about $10^{-8.5}$ mol l⁻¹) has been determined experimentally by γ irradiation,⁴ which gives no indication of the status of the ion pair (intimate/dissociated). Our simulations deal with a concentration of about 5×10^{-2} mol l⁻¹, that is, to supersaturated conditions. There might thus be some concentration effects on the solvation properties of the cation *vs.* the anion. On the other hand, our results point out the importance of solvent interactions in the first shells, which should be less dependent on the concentration, if the ions are dissociated.

Concerning the computations, a quantitative assessment of solvation features and thermodynamic properties certainly requires that the energy representation of the system (ions and solvents) and an “adequate” treatment of electrostatic and internal interactions⁵² (especially with an explicit representation of non-additivity and polarization effects^{53,54}) be tested. In the case of the spherical S^+ and S^- model species, there is no problem of charge distribution in the solute, whose periphery is “inert”. However, quite large differences in solvation properties are found, especially in water, leading to marked differences in free energies of transfer to chloroform or to acetonitrile. In the case of $\text{B}\phi_4^-$ and $\text{As}\phi_4^+$ ions, the electrostatic representation is not unique. Even in well-documented examples of small molecules involving C, H, O, N atoms only there is no *a priori* “best choice of charges”. The latter are tested on experimental quantities, including free energies of solvation,⁵⁵ which are not available from experiment for the *individual* $\text{B}\phi_4^-$ and $\text{As}\phi_4^+$ ions. The charges chosen in this study were derived consistently from ESP calculations, but other sets may be derived and repeatedly tested in various solutions. We notice that three other sets of charges (and particularly set-2, which models the periphery of ions as perfectly “inert”) lead qualitatively to the same conclusions concerning the importance of sign reversal on differences in free energies of solvation of large symmetrical ions. Other critical parameters for this study are those of the solvents, which were derived from pure liquid phase properties, and may not be accurate enough to describe their mutual competition with the solutes properly. It remains that the two models of tetrahedral or two spherical ions interact very differently with a given model of solvent. Three different models of chloroform give the same trends. We are currently investigating other models of solvents and modified treatments of the long-range electrostatic interactions. Further improvements involve a mixed MM/QM description of the potential energy,^{56,57} which again raise the question of a balanced description of the two ions. In principle, annihilation of the $\text{B}\phi_4^-\text{As}\phi_4^+$ pair in the different solvents should allow one to compare the differences in total solvation energies from one solvent to the other. This introduces new computational problems, due to the large size of the solute, as well

as physical problems, related to the effect of concentration on the status of the ion pair as a function of the solvent.

Our computational results are disturbing in many respects, if one refers to classical representations of large hydrophobic ions in solution. Contrary to assumptions made in the TATB hypothesis, these ions are calculated to display marked differences of solvation properties, which depend on the sign of the ionic charge, the nature, hydrogen bonding capabilities and polarity of the solvent. In addition, the precise *shape* of the ion matters, as tetrahedral ions may display the opposite behaviour compared to spherical ones. As the granularity of the solvent plays an important role (even around the large spherical ions), the latter cannot be modelled solely by a continuum. Our study should stimulate further theoretical treatments along the line described above, as well as experiments on the effect of the charge of ions and properties in solution. Fundamentally, they have bearing on our understanding of the hydrophilic/hydrophobic character of neutral and large ionic solutes^{58,59} and on their behaviour at aqueous interfaces.^{60–69} Such computations will play an increasing role in the critical analysis of the thermodynamics of solvation and transfer of ions.

Acknowledgements

The authors are grateful to IDRIS and Université Louis Pasteur for computer resources and to PRACTIS for support. RS thanks the French Ministry of Research for a grant.

Notes and references

- 1 R. A. Robinson and R. H. Stokes, *Electrolyte Solutions*, Butterworths, London, 1955, ch. 3.
- 2 A. Ben-Naim and Y. Marcus, *J. Chem. Phys.*, 1984, **81**, 2016.
- 3 N. Bjerrum and E. Larsson, *Z. Phys. Chem.*, 1927, **127**, 358.
- 4 J. I. Kim, *J. Phys. Chem.*, 1978, **82**, 191.
- 5 Y. Marcus, *Ion Solvation*, Wiley, Chichester, 1985.
- 6 Y. Marcus, *Pure Appl. Chem.*, 1990, **62**, 900.
- 7 E. Grunwald, G. Baughman and G. Kohnstam, *J. Am. Chem. Soc.*, 1960, **82**, 5801.
- 8 O. Popovych, *Anal. Chem.*, 1966, **38**, 558.
- 9 R. Alexander and A. J. Parker, *J. Am. Chem. Soc.*, 1967, **89**, 5549.
- 10 Y. Marcus, *J. Chem. Soc., Faraday Trans. 1*, 1987, **83**, 2985.
- 11 A. D. Buckingham, *Discuss. Faraday Soc.*, 1957, **24**, 151.
- 12 R. A. Pierotti, *Chem. Rev.*, 1976, **76**, 717.
- 13 M. Prévost, I. T. Oliveira, J. P. Kocher and S. J. Wodak, *J. Phys. Chem.*, 1996, **100**, 2738.
- 14 D. A. Pearlman, D. A. Case, J. C. Caldwell, G. L. Seibel, U. C. Singh, P. Weiner and P. A. Kollman, AMBER4, University of California, San Francisco, 1991.
- 15 W. D. Cornell, P. Cieplak, C. I. Bayly, I. R. Gould, K. M. Merz, D. M. Ferguson, D. C. Spellmeyer, T. Fox, J. W. Caldwell and P. A. Kollman, *J. Am. Chem. Soc.*, 1995, **117**, 5179.
- 16 W. L. Jorgensen, J. Chandrasekhar and J. D. Madura, *J. Chem. Phys.*, 1983, **79**, 926.
- 17 W. L. Jorgensen, J. M. Briggs and M. L. Contreras, *J. Phys. Chem.*, 1990, **94**, 1683.
- 18 P. A. Kollman, *Acc. Chem. Res.*, 1996, **29**, 461.
- 19 The importance of electrostatics is further demonstrated by additional simulations of both ions repeated in a "polar" chloroform model, where the OPLS charges have been scaled by 1.3. This increases the interaction energies of the solvent with $\text{B}\phi_4^-$ and $\text{As}\phi_4^+$, relative to the unscaled OPLS charges, and also the difference in "solvation energies" of the two ions ($\Delta E_{\text{ss}} = 32 \pm 5$ kcal mol⁻¹).
- 20 S. Boudon, G. Wipff and B. Maigret, *J. Phys. Chem.*, 1990, **94**, 6056.
- 21 L. Troxler, J. M. Harrowfield and G. Wipff, *J. Phys. Chem.*, 1998, **102**, 6821.
- 22 I. Dance and M. Scudder, *Chem. Eur. J.*, 1996, **2**, 481.
- 23 I. Dance and M. Scudder, *J. Chem. Soc., Dalton Trans.*, 1996, 3755.
- 24 G. A. Jeffrey, *Acc. Chem. Res.*, 1969, **2**, 344.
- 25 G. A. Jeffrey and W. Saenger, *Hydrogen Bonding in Biological Structures*, Springer-Verlag, Berlin, 1991.
- 26 G. A. Jeffrey, in *Inclusion Compounds*, ed. J. L. Atwood, J. E. D. Davies and D. D. MacNicol, Academic Press, London, 1984, pp. 135–190.
- 27 J. Lipkowski, in *Comprehensive Supramolecular Chemistry*, ed. D. D. MacNicol, F. Toda and R. Bishop, Pergamon, New York, 1996, pp. 691–714.
- 28 J. Lipkowski, in *Crystallography of Supramolecular Compounds*, ed. G. Tsoucaris, Kluwer Academic Publishers, Dordrecht, 1995, pp. 265–283.
- 29 A. W. Adamson, *Physical Chemistry of Surfaces*, 5th edn., Wiley, New York, 1990.
- 30 T. P. Straatsma and J. A. McCammon, *Annu. Rev. Phys. Chem.*, 1992, **43**, 407.
- 31 W. L. Jorgensen, *Acc. Chem. Res.*, 1989, **22**, 184.
- 32 B. Guillot, Y. Guissani and S. Bratos, *J. Chem. Phys.*, 1991, **95**, 3643.
- 33 The $\Delta G_{\text{wat}}^{+-}$ values are close to those expected from the Born model (-30 kcal mol⁻¹), whereas the $\Delta G_{\text{wat}}^{0-}$ values might seem surprisingly low. We checked on the reverse mutation S^- to S^0 that the sampling was sufficient ($\Delta G_{\text{wat}}^{0-} = +13.7$ kcal mol⁻¹, nearly identical to $-\Delta G_{\text{wat}}^{0+}$).
- 34 Due to the finite size of the simulated system, the ΔG s are evaluated within the cutoff distance and the contributions beyond this distance may not be the same for steps 1 to 3. The first series of tests concern the increase from a 11 Å cutoff to a 11/15 Å twin cutoff. In the case of water solutions of tetrahedral and spherical species, this somewhat reduces ΔG^{+-} (by less than 1.5 kcal mol⁻¹), and its ΔG^{0-} and ΔG^{0+} components. The question of sampling was checked on the first half of the $\text{B}\phi_4^-$ to $\text{B}\phi_4^0$ mutation in water ($\text{B}\phi_4^-$ to $\text{B}\phi_4^{-0.5}$), which displays the largest ΔG s, compared to the other systems (Table 6). The results obtained with 21, 51 and 101 windows, using a 11 Å cutoff, were very close (34.8, 34.5 and 34.0 ± 0.2 kcal mol⁻¹, respectively), indicating that there is no major sampling problem when using 21 windows only per mutation.
- 35 R.-S. Tsai, W. Fan, N. El Tayar, P. A. Carrupt, B. Testa and L. B. Kier, *J. Am. Chem. Soc.*, 1993, **115**, 9632.
- 36 T. Osakai, A. Ogata and K. Ebina, *J. Phys. Chem. B*, 1997, **101**, 8341.
- 37 As $\Delta G_{\text{chlor}}^{+-}$ critically determines the difference in free energies of transfer, we made two other estimates of this quantity. The first one used a more polar model of chloroform, where the OPLS charges were scaled by 1.3. For the direct mutation of $\text{As}\phi_4^+$ to $\text{B}\phi_4^-$ (51 windows and 15 Å cutoff), $\Delta G_{\text{chlor}}^{+-}$ becomes more negative than with the OPLS charges (-15.7 versus -12.3 kcal mol⁻¹). The second test was performed using an all-atom model of chloroform (from ref. 53) and a 15 Å cutoff. All ΔG s were similar to those obtained with the OPLS model (Table 6). In particular, $\Delta G_{\text{chlor}}^{+-}$ was -13.2 instead of -14.6 kcal mol⁻¹ (i.e., still more negative than $\Delta G_{\text{wat}}^{+-}$). Thus, these tests strengthen the above conclusion that $\text{B}\phi_4^-$ is more easily transferred to chloroform than $\text{As}\phi_4^+$.
- 38 J. Stangret and E. Kamińska-Piotrowics, *J. Chem. Soc., Faraday Trans.*, 1997, **93**, 3463.
- 39 P. K. Bakshi, A. Linden, B. R. Vincent, S. P. Roe and D. Adhikar, *Can. J. Chem.*, 1973, **72**, 1273.
- 40 P. K. Bakshi, *Can. J. Chem.*, 1994, **72**, 1273.
- 41 Y. Marcus, *Pure Appl. Chem.*, 1987, **9**, 1093.
- 42 M. H. Abraham and J. Liszi, *J. Inorg. Nucl. Chem.*, 1981, **43**, 143.
- 43 B. Roux, H.-A. Yu and M. Karplus, *J. Phys. Chem.*, 1990, **94**, 4683.
- 44 M. Schaefer and M. Karplus, *J. Phys. Chem.*, 1996, **100**, 1578.
- 45 A. Warshel and S. T. Russell, *Quart. Rev. Biophys.*, 1984, **17**, 283.
- 46 A. A. Rashin, *J. Phys. Chem.*, 1989, **93**, 4664.
- 47 J. Åqvist and T. Hansson, *J. Phys. Chem.*, 1996, **100**, 9512.
- 48 V. Luzhkov and A. Warshel, *J. Comput. Chem.*, 1992, **13**, 199.
- 49 K. J. Schweighofer and I. Benjamin, *J. Phys. Chem.*, 1995, **99**, 9974.
- 50 S. E. Jackson and M. C. R. Symons, *Chem. Phys. Lett.*, 1976, **37**, 551.
- 51 Y. Shao, A. A. Stewart and H. H. Girault, *J. Chem. Soc., Faraday Trans.*, 1991, **87**, 2593.
- 52 X. Daura, P. H. Hünenberger, A. E. Mark, E. Querol, F. X. Avilés and W. F. van Gunsteren, *J. Am. Chem. Soc.*, 1996, **118**, 6285.
- 53 T.-M. Chang, K. X. Dang and K. A. Peterson, *J. Phys. Chem. B*, 1997, **101**, 3413.
- 54 M. H. New and B. J. Berne, *J. Am. Chem. Soc.*, 1995, **117**, 7172.
- 55 G. Kaminski and W. L. Jorgensen, *J. Phys. Chem.*, 1996, **100**, 18010.
- 56 J. Gao, *Acc. Chem. Res.*, 1996, **29**, 298.
- 57 M. A. Thompson, E. D. Glendening and D. Feller, *J. Am. Chem. Soc.*, 1994, **116**, 10465.
- 58 B. G. Rao and U. C. Singh, *J. Am. Chem. Soc.*, 1989, **111**, 3125.

- 59 W. Blokzijl and J. B. F. N. Engberts, *Angew. Chem., Int. Ed. Engl.*, 1993, **32**, 1545.
- 60 R. Bennes and B. E. Conway, *Can. J. Chem.*, 1981, **59**, 1978.
- 61 W. A. Ducker and L. M. Grant, *J. Phys. Chem.*, 1996, **100**, 11 507.
- 62 M. Hato, *J. Phys. Chem.*, 1996, **100**, 18 530.
- 63 C. Y. Lee, J. A. McCammon and P. J. Rossky, *J. Chem. Phys.*, 1984, **80**, 4448.
- 64 J. S. Nowick, J. S. Chen and G. Noronha, *J. Am. Chem. Soc.*, 1993, **115**, 7636.
- 65 A. R. van Buuren, S.-J. Marrink and J. C. Berendsen, *Colloids Surf.*, 1995, **102**, 143.
- 66 F. Berny, N. Muzet, R. Schurhammer, L. Troxler and G. Wipff, in *Current Challenges in Supramolecular Assemblies*, ed. G. Tsoucaris, Kluwer Academic Publishers, Dordrecht, 1998, pp. 221–248.
- 67 F. Berny, N. Muzet, L. Troxler and G. Wipff, in *Supramolecular Science: Where It Is and Where It Is Going*, ed. R. Ungaro and E. Dalcanele, Kluwer Academic Publishers, Dordrecht, 1999, pp. 95–125.
- 68 M. Lauterbach, E. Engler, N. Muzet, L. Troxler and G. Wipff, *J. Phys. Chem. B*, 1998, **102**, 225.
- 69 N. Muzet, E. Engler and G. Wipff, *J. Phys. Chem. B*, 1998, **102**, 10 772.

Paper 9/00442D